Modeling the anaerobic treatment of sulfate-rich urban wastewater: application to AnMBR technology

Freddy Durán [a], Ángel Robles[b,1], Juan Bautista Giménez[a], José Ferrer[a], Josep Ribes [b], Joaquín Serralta [a]

[a] CALAGUA – Unidad Mixta UV-UPV, Institut Universitari d'Investigació d'Enginyeria de l'Aigua i Medi Ambient – IIAMA, Universitat Politècnica de València, Camí de Vera s/n, 46022, València, Spain.

[b]CALAGUA – Unidad Mixta UV-UPV, Departament d'Enginyeria Química, Universitat de València, Avinguda de la Universitat s/n, 46100, Burjassot, València, Spain

1.1. Abstract

Although anaerobic membrane bioreactors (AnMBR) are a core technology in the transition of urban wastewater (UWW) treatment towards a circular economy, the transition is being held back by a number of bottlenecks. The dissolved methane released from the effluent, the need to remove nutrients (ideally by recovery), or the energy lost by the competition between methanogenic and sulfate-reducing bacteria (SRB) for the biodegradable COD have been identified as the main issues to be addressed before AnMBR becomes widespread. Mathematical modeling of this technology can be used to obtain further insights into these bottlenecks plus other valuable information for design, simulation and control purposes. This paper therefore proposes an AnMBR anaerobic digestion model to simulate the crucial SRB-related process since these bacteria degrade more than 40% of the organic matter. The proposed model, which is included in the BNRM2 collection model, has a reduced but all-inclusive structure, including hydrolysis, acidogenesis, acetogenesis, methanogenesis and other SRB-related processes. It was calibrated and validated using data from an AnMBR pilot plant treating sulfate-rich UWW, including parameter values obtained in off-line experiments and optimization methods. Despite the complex operating dynamics and influent composition, it was able to reproduce the process performance. In fact, it

[1] Corresponding author: angel.robles@uv.es

was able to simulate the AD of sulfate-rich UWW considering only two groups of SRB: heterotrophic SRB growing on both VFA (propionate) and acetate, and autotrophic SRB growing on hydrogen. Besides the above-mentioned constraints, the model reproduced the dynamics of the mixed liquor solids concentration, which helped to integrate biochemical and filtration models. It also reproduced the alkalinity and pH dynamics in the mixed liquor required for assessing the effect of chemical precipitation on membrane scaling.

1.2. Keywords

Anaerobic membrane bioreactor; BNRM2; modeling; sulfate-rich urban wastewater

2. Introduction

Anaerobic membrane bioreactors (AnMBR) have attracted attention to drive the shift of urban wastewater (UWW) treatment towards the circular economy. This technology combines the advantages of anaerobic systems with membrane filtration: i) it retains 100% of particulate materials, allowing accurate control of the sludge retention time (SRT) thus preventing slow-growing methane-forming methanogens to be washed out of the system while producing high quality solids- and pathogen-free effluent; ii) it enables AD to be operated at ambient-temperatures by increasing the SRT; iii) it reduces biosolid waste because of the lower biomass yields of anaerobic microorganisms; and iv) it transforms organics into a gaseous energy carrier CH_4 (Lei et al., 2018; Maaz et al., 2019; Robles et al., 2018a; Shin and Bae, 2018). AnMBR does not destroy nutrients and produces a nutrient-loaded, high-quality effluent useful for nutrient recovery (e.g. struvite crystallization, microalgae cultivation and fertirrigation, among others) (Chen, 2020; Guo et al., 2016; Raskin et al., 2012). Indeed, optimizing AnMBR design and operations by the assessment of environmental, economic and technological trade-offs enables AD to be operated cost-effectively with a significant reduction in costs and environmental impact while being a net energy producer, unlike conventional aerobic UWW treatments combined with waste sludge AD (Mei et al., 2016; Pretel et al., 2016). However, this application still presents some issues that need further consideration,

such as: i) the methane concentration dissolved in the effluent, which has to be captured to maximize energy harvesting and avoid direct greenhouse gas (GHG) emissions downstream (Cookney et al., 2016; Crone et al., 2016; Sanchis-Perucho et al., 2020); ii) the need for a post-treatment step for nutrient recovery within the circular economy (Robles et al., 2019a; Ye et al., 2020); or iii) the reduced energy harvested due to the competition between methanogens and sulfate-reducing bacteria (SRB) for the available substrate when treating UWW with low biodegradable organics-to-sulfate ratios (BOD:$SO4^{2-}$-S) (see e.g. Giménez et al., 2012b; Lens et al., 1998a; Pretel et al., 2014). Although AnMBR has been put forward as a core technology for the sustainable treatment of different waste streams, it is necessary to thoroughly explore the role and impact of its drawbacks before its widespread application. AnMBR modeling can offer a number of advantages in this field, including the analysis of technical, economic and environmental feasibility, technology development, or model-based design. Since it has not yet been implemented full-scale for UWW treatment, the design issues are particularly important as they finally determine capital costs, operating costs and technical viability.

Anaerobic digestion (AD) modeling is a mature field largely guided by mechanistic model structures defined by understanding the underlying processes (Batstone et al., 2015). The most widely used AD model to describe sludge stabilization is the well-known IWA ADM1 (Batstone et al., 2002), which has been applied to modeling a large number of AD processes (Donoso-bravo et al., 2011). However, the model calibration and validation can be somewhat complex for modeling certain substrates.

The modeling goal should define the complexity level of the model to be selected in order to obtain useful information (Donoso-bravo et al., 2011), *e.g.* understanding metabolic pathways, evaluating effluent quality, assessing biogas production and quality, evaluating membrane fouling, etc. For instance, simulating methane production or effluent quality in a system treating low-strength wastewater such as UWW may require less data on the metabolic pathways for organic degradation than the treatment of high-strength wastewaters, while the degradation of more complex substrates (*e.g.* food waste) could require expanded existing models. One issue of AD modeling deals with selecting and adapting models

capable of reproducing the performance of new anaerobic processes such as AnMBR (Robles et al., 2018b). The model parameters should be optimized specifically for AnMBR technology, since membrane filtration can control SRT while modifying the organic loading rate (OLR), thus affecting the limiting or controlling mechanisms during AD. Data from an existing AnMBR system would allow specific parameters to be tuned. Also, well-balanced model complexity and usability is essential for AnMBRs, e.g. one of the key issues is the type of particle treated (i.e., biomass and solid substrate), since it affects membrane performance. The kinetic structure of the biological model should be relatively simple (at least two-step) but complex enough to represent the behavior of the particles in the system (Batstone, 2006).

Different modifications are available for adapting ADM1 to different processes (Batstone et al., 2006, Zaher et al., 2007, Kythreotou et al., 2014,Batstone et al., 2015). Several authors have proposed simpler modeling approaches, e.g. Charfi et al. (2017) developed a mathematical model for AnMBR simulation coupling a simplified anaerobic model and another for membrane fouling. The BNRM2 collection model proposed by Barat et al. (2013) incorporates a simplification of ADM1 in a general model linked to a an AnMBR filtration model (Robles et al. 2013b), although sulfate-reducing processes are not incorporated in Barat et al. (2013). BNRM2 considers the most important physical, chemical and biological processes taking place in WWTPs. The physical processes considered are: sedimentation and gas liquid transfer and the chemical are: acid base reactions considered as equilibrium governed processes and precipitation and redissolution processes. The bacterial groups considered are: heterotrophic, two groups of ammonium oxidizing (k-strategist and r-strategist), nitrite oxidizing, polyphosphate accumulating, acidogenic, acetogenic and two groups of methanogenic (acetotrophic and hydrogenotrophic). Copp et al. (2005) presented an AD sub-model model extracted from the Mantis collection model on GPS-X software which also includes an AnMBR module. Aquino and Stuckey (2008) incorporated soluble microbial products (SMPs) and extracellular polymeric substances (EPSs) in a reduced model architecture due to the accumulation of SMPs inside AD systems and their effect on other downstream processes such as membrane filtration. The AM2b anaerobic model proposed by Benyahia et al. (2013) –

a modification of the simple two-step AM2 model (Bernard et al., 2001) – incorporates SMP production and degradation pathways to allow integration with a filtration sub-model. However, anaerobic models applied to AnMBRs are usually developed or validated for the treatment of high-strength wastewater.

Modeling the amount of methane dissolved in the effluent is essential to evaluate and optimize the economic and environmental feasibility of AD systems for sewage treatment, especially when operating at low temperatures since the amount of methane that is lost in the effluent can increase by up to 80% when operating at temperatures below 15 ºC (Giménez et al., 2014). A post-treatment step for nutrient removal and/or recovery might be needed, depending on the sensitivity of the receiving water body. Accurately determining effluent quality is thus essential for designing classical or advanced techniques for nutrient removal or recovery, such as an ammox process, membrane contactors, bioelectrochemical systems, microalgae cultivation, phototrophic bacteria cultivation, fertirrigation, ion exchange, ammonia stripping, etc. (Robles et al., 2019).

Modeling sulfate reduction in AD systems is also essential to assess UWW methane production with low biodegradable organics to sulfate ratios (BOD:SO_4^{2-}-S), where competition between methanotrophs and SRB may be a key phenomenon. The most popular anaerobic models dealing with SRB are usually complex, and the information contained in parameter values and model structure does not translate well to simple design rules (Batstone, 2006). Other authors have modeled these processes at lower complexity levels by proposing different numbers of SRB activities and electron donors (Cassidy et al., 2015). As commented before, selecting complexity levels depends on the modeling goal (*e.g.* understanding metabolic pathways, or evaluating biogas production and quality). For instance, different models with a limited number of SRB pathways have been proposed to simulate the competition between methanogens and SRB for acetate (Fomichev and Vavilin, 1997), acetate and hydrogen (Ahammad et al., 2011,Harerimana et al., 2013), or simply hydrogen (Batstone, 2006). Increasing the number of SRB pathways, Knobel and Lewis (2002) considered five groups of SRB consuming butyrate,

lactate, propionate, acetate and hydrogen; Frunzo et al. (2012) also considered five groups of microbes (heterotrophic SRB, autotrophic SRB, homoacetogenic bacteria, methanogenic archaea, and acetate-degrading bacteria); and Kalyuzhnyi and Fedorovich (1998) proposed seven SRB groups. Up to four SRB groups consuming butyrate, propionate, acetate and hydrogen were incorporated in the ADM1 by (Ahmed and Rodríguez, 2018, 2017, Barrera et al., 2015, Fedorovich et al., 2003) and most of these models were developed and validated in AD systems treating high-strength wastewaters.

Due to the low BOD:SO_4^{2-}-S, SRB modeling is essential for mainstream AD technology development. Although Fedorovich et al. (2003) and other authors have presented useful extensions to the ADM1 for sulfate reduction, these extensions usually include several processes that complicate model implementation and usability, apart from having been developed for high-strength wastewater. Indeed, the simplification proposed by Batstone et al. (2002) aims to avoid these complexities by assessing sulfate reduction and only considering the oxidation of available hydrogen by adding hydrogen and bicarbonate as separate states. This simplified approach was validated at SO_4^{2-}-S:BOD ratios of up to approximately 0.1 $gS \cdot g^{-1}COD$, after which hydrogen is depleted. At higher SO_4^{2-}-S:BOD ratios, SRB starts to oxidize organic acids, and other metabolic pathways are needed. Thus, a compromise between complexity and usability is needed for modeling mainstream AD systems treating wastewaters characterized by low BOD:SO_4^{2-}–S ratios, such as sulfate-rich UWW.

It is also necessary to adequately reproduce physicochemical dynamics (e.g. gas flow, chemical equilibrium and pH calculation) in order to account for other processes affecting AnMBR, such as chemical precipitation and membrane scaling. In contrast to other AD systems, gas-assisted AnMBR systems are usually operated under gas-saturation, so that gas flow calculations are essential to evaluate the dissolved gas content in the effluent. Dissolved methane should be recovered in downstream processes to enhance the viability of full-scale AnMBR for UWW treatment. Apart from biogas production, adequate representation of saturation and oversaturation of liquid streams is essential in mainstream AD

processes. pH has a strong impact on carbon dioxide transfer, mineral solids precipitation and biological conversions. The concentrations of ionic species (acids and bases) in equilibrium with ionic, active state variables can also be calculated. From this equilibrium, precipitation calculations are possible, which is essential to evaluate problems related to membrane scaling or the potential nutrient recovery from the effluent in downstream processes. Therefore, comprehensive pH and equilibrium prediction is needed to evaluate the feasibility of different treatment platforms for resource recovery.

Deepening the understanding of the mechanistic processes involved could also expand AnMBR applicability to address new challenges, such as combining AnMBR with other technologies for the recovery of resources, and it is expected to be combined with new or existing technologies for UWW treatment (e.g. primary settling, activated sludge processes for nutrient removal, etc.). The integration of AnMBR anaerobic models into plant-wide or collection models would help to develop new resource recovery platforms, which would assist in selecting the best treatment scheme and optimal operational conditions by considering a variety of technological solutions for resource recovery and nutrients removal (Seco et al., 2020). For example, Solon et al. (2019) evaluated the effects on plant performance of combining techniques to recover resources from wastewater. Other examples are available setting down the rules to assist in the conception and design of new schemes (Fernández-Arévalo et al., 2017; Lizarralde et al., 2019; Martí et al., 2017).Different studies are also available comparing this technology with conventional technologies. For instance, Pretel et al. (2016) contrasted the performance of an AnMBR combined with a nutrient-removal post-treatment with different aerobic-based wastewater treatment schemes using a plant-wide model. Becker et al. (2017) put forward AnMBR and high-rate activated sludge (HRAS) combined with AD for the co-digestion of domestic wastewater and food waste. Last, but not least, adequate resource recovery modeling platforms would help (model-based) control development of non-linear processes, making it possible to develop and test new control and optimization strategies.

Although BNRM2 is a collection model, it fails to simulate the AnMBR performance when treating sulfate-

rich UWW. In this case, the model overestimates methane production since the SRB are not considered. In this context, this paper proposes the BNRM2S, a modified version of the BNRM2 plant-wide model (Barat et al., 2013), which can be applied to different anaerobic systems for sulfate-rich UWW treatment, such as AnMBR. BNRM2 has a reduced comprehensive structure for the anaerobic degradation of organics, including hydrolysis, acidogenesis, acetogenesis, methanogenesis and the effect of influent sulfate on process performance. The model is implemented on DESASS software (Ferrer et al., 2008) and was calibrated and validated by data from an AnMBR plant with industrial-scale membranes. The paper also gives an overview of current and future challenges in AnMBR modeling.

3. Material and methods

3.1. AnMBR pilot plant

The proposed model was calibrated and validated by data from an AnMBR pilot plant at the "Barranco del Carraixet" WWTP in Alboraya (Valencia), Spain. The AnMBR consisted of a 1.3 m^3 jacketed anaerobic reactor connected to two 0.8 m^3 membrane tanks. Each membrane tank included one commercial ultrafiltration hollow-fiber membrane system (KMS, PUR-PSH31, 0.03-µm pores, 31-m^2 filtration area). A rotofilter with a screen size of 0.5 mm was installed as pre-treatment. One equalization tank (0.3 m^3) and one Clean-In-Place tank (0.2 m^3) were also included as main elements of the pilot plant. A fraction of the produced biogas was continuously recycled to the anaerobic reactor in order to improve the stirring conditions and to favor stripping the produced gases from the liquid phase, while another fraction was continuously recycled to the bottom of the hollow-fiber membranes to minimize cake layer formation. A degassing vessel was installed between each membrane tank and its vacuum pump to recover bubbles of biogas in the permeate. A temperature control system was implemented consisting of a warm-water tank equipped with a 6 kW heater and a thermostat that maintained the water at 65 ºC. When necessary, the temperature in the anaerobic reactor was controlled by a water pump that enabled the warm water to flow through the reactor jacket according to the difference between the reactor and set point temperatures. Further details of this AnMBR pilot plant can be found in Giménez et al. (2011).

3.2. AnMBR pilot plant monitoring

Different on-line sensors and monitoring equipment were installed in the plant to obtain real-time information on the state of the process, such as: gas-flow-rate transmitters (vortex type) in the gas inlets to anaerobic reactor and membrane tanks; one gas pressure transmitter (gauge pressure type), which monitored the gas pressure in the head of the reactor; one pH-T and one ORP sensor in the anaerobic reactor internal sludge recycling; one biogas analyzer to monitor biogas composition (CH_4, CO_2, H_2 and H_2S); and one gas meter (pulse measurement) to monitor biogas production.

Besides the on-line process monitoring, the following parameters were determined to monitor plant performance: total and soluble COD (COD_T and COD_S), total nitrogen (N_T) and total phosphorus (P_T) were determined once a week; total and volatile solids (TS and VS), total and volatile suspended solids (TSS and VSS), volatile fatty acids (VFA), alkalinity (Alk), sulfate (SO_4^{2-}), sulfide (HS^-), total nitrogen (N_T), total phosphorus (P_T), ammonium (NH_4^+), and phosphate (PO_4^{3-}) were determined three times a week. 24-hour-composite samples were taken from influent and effluent streams. Grab samples were taken from the mixed liquor.

3.3. Analytical methods

COD_T, COD_S, TS, VS, TSS, VSS, SO_4^{2-} (turbidimetric method 4500-SO_4^{2-} E), HS^- (methylene blue method, 4500-S^{2-} D), P_T (Persulfate digestion method, 4500-P B.5, followed by ascorbic acid colorimetric method, 4500-P F), NH_4^+ (authomated phenate method, 4500-NH_3 G) and PO_4^{3-} (ascorbic acid colorimetric method, 4500-P F) were determined according to Standard Methods (APHA, 2005). N_T was determined with commercial total nitrogen cell tests (114537 Merck Millipore), VFA and Alk concentration was determined by titration according to the method proposed by Moosbrugger et al. (1992). The concentration of dissolved methane in the effluent was indirectly determined through the static-headspace gas chromatography analysis technique described by Giménez et al. (2012b). Biogas

composition was monitored with an Emmerson Process Analytical Gmbh X-stream multiple purpose multiparametric gas analyzer after sample conditioning. Non-dispersive Infrared and ultraviolet, and termoconductivity analyzers were used for CH_4 and CO_2, H_2, and H_2S, respectively.

3.4. AnMBR plant operation

The plant was continuously operated for 2.5 years with effluent from the pre-treatment of the "Carraixet" full-scale WWTP (València, Spain). The pre-treatment step of the full-scale facility consisted of screening and sand and grease removal. After an additional pre-treatment of the wastewater in a sieve screw and homogenization in an equalization tank, the wastewater was pumped to the anaerobic reactor. The average characterization of the influent during the experimental period is shown in Table 1. The influent wastewater was characterized by a notably low BOD:SO_4^{2-}S ratio (mean 3.6 ± 1.97 kg BOD·kg^{-1} SO_4-S), as well as a highly variable load, which enabled calibrating and validating model performance under a wide range of influent conditions. Figure 1 shows the evolution during the experimental period of the SRT, the hydraulic retention time (HRT), and the temperature. As this figure shows, the entire experimental period was divided into 13 operating periods (periods I to XIII), in which the operating conditions were: SRT 20 – 70 days, OLR 0.5 – 2 kg COD $m^3 \cdot d^{-1}$, and HRT 5 – 24 hours. Temperature ranged from 14 to 33 ºC. The AnMBR was firstly operated at a controlled temperature of 33 and 20 ºC (days 1-150 and 200-400, respectively), while the system was mostly operated at ambient temperature (the temperature controller was switched-off) from day 400 to the end of the experimental period (see Figure 1). An in-depth analysis of the experimental data used in this study can be found in Giménez et al. (2014, 2012a, 2012b, 2011).

The mixed liquor from the anaerobic reactor was continuously recycled through the membrane tanks, in which the effluent was obtained by vacuum filtration. A fraction of the biogas produced in the system was recycled to the reactor for stirring purposes through fine bubble diffusers. Biogas recycling flow to the reactor was around 0.5 Nm^3 per m^3 of working volume. Another fraction was recycled to the membrane

tanks for membrane scouring for its additional gas stripping effect. The specific gas demand per membrane area was around 0.2-0.3 Nm^3/h per m^2 of membrane. Further details on membrane performance can be found elsewhere (see e.g. Robles et al., 2014). This stirring strategy favored the mass-transfer of dissolved gases between the liquid and gas phases, thus avoiding oversaturation of methane in the effluent (Giménez et al., 2012b).

3.5. Model description

This paper describes an extended version of the AD sub-model included in the BNRM2 collection model (Barat et al., 2013), including SRB-related processes. The AD sub-model has a reduced but comprehensive structure based on hydrolysis, acidogenesis, acetogenesis and methanogenesis. All the model components and model notations are defined following the standard nomenclature proposed by Corominas et al. (2010).

The soluble components considered in the AD sub-model are the following: fermentable readily biodegradable substrate not including VFA (S_F), fermentation products expressed as propionate excluding acetate (S_{VFA}), acetate (S_{Ac}), dissolved hydrogen (S_{H2}), dissolved methane (S_{CH4}), total inorganic carbon consisting of CO_2, HCO_3^- and CO_3^{2-}($S_{Ig,C}$), inert soluble organic material (S_U), total proton concentration including free protons and those associated with acidic components (S_H), ammonium plus ammonia nitrogen (S_{NHx}), and orthophosphates (S_{PO4}). Minteqa2 is used to calculate the equilibrium, which includes the calculation of ionic species. The particulate components considered are the following: inert particulate organic material (X_U), particulate biodegradable organic material (XC_B), acidogenic bacteria (X_{AO}), acetogenic bacteria (X_{PRO}), methanogenic acetoclastic organisms (X_{ACO}), methanogenic hydrogenotrophic organisms (X_{HMO}) and total suspended solids (X_{TSS}).Due to the reduced complexity of the substrate to be consumed (sulfate-rich UWW), only two groups of SRB were considered: heterotrophic SRB growing on both VFA (propionate) and acetate, and autotrophic SRB growing on hydrogen. As regards sulfate-reducing processes, the extended BNRM2S model considers 4

new components split into 2 soluble and 2 particulates: sulfate (S_{SO4}), total sulfide (S_S), heterotrophic SRB (X_{HSRO}) and autotrophic SRB (X_{ASRO}). Only one group of heterotrophic SRB was considered, since it was demonstrated in batch experiments (data not shown) that the SRB that degrade both substrates should be considered as the same bacterial group. SRB that degrade fermentable readily biodegradable substrates (S_F) were not considered since acidogenic bacteria outcompete this bacterial group (Widdel, 1988). Only two groups of SRB were therefore introduced in the model. Heterotrophic SRB are able to grow on acetate and propionate. The catabolic reactions are shown in Eqs. (1) and (2)

$$CH_3COOH + SO_4^{2-} \rightarrow 2CO_2 + 2\,H_2O + S^{2-} \quad \text{(Eq. 1)}$$

$$CH_3CH_2COOH + 7/4\ SO_4^{2-} \rightarrow 3\ CO_2 + 3\ H_2O + 7/4\ S^{2-} \quad \text{(Eq. 2)}$$

Since the extended model is able to calculate H_2S concentration, a non-competitive inhibition term for this species was included in the kinetic expression of every growth process.

Figure 2 shows a schematic representation of the biochemical processes included in the AD model extracted from the BNRM2S collection model, including sulfate-reducing processes. The stoichiometry of the anaerobic sub-model included in BNRM2S and the conversion factors to be applied to the continuity equations of the model for N, P, mass, carbon and proton are available as e-supplementary material (Table S1 and Table S2). The kinetic expressions of the anaerobic sub-model in BNRM2S are also provided as e-supplementary material (Table S3). A surface-limited reaction was assumed for the kinetic expressions of the hydrolysis process, as usually considered in activated sludge models. Monod terms are used to model the growth limitation for substrate, electron acceptor and nutrients. Non-competitive inhibition terms were used to model thermodynamic inhibitions (high hydrogen concentrations reduce the fermentation rate) as well as the microbial inhibitions (growth rate of all the bacterial groups are affected by the presence of hydrogen sulfide). Since it is assumed that S_{VFA} and S_A are consumed simultaneously by SRB, competitive inhibition terms were included in the corresponding kinetic expressions. The pH inhibition function denoted by I_{pH1} consists of a combination of classical Monod and non-competitive

inhibition switching functions (Barat et al., 2013; Seco et al., 2004) (Eq. 3).

$$I_{pH1} = \frac{\frac{S_{[H]}}{K_{S,H} + S_{[H]}} \cdot \frac{K_{I,H}}{K_{I,H} + S_{[H]}}}{\frac{S_{[H],Opt}}{K_{S,H} + S_{[H],Opt}} \cdot \frac{K_{I,H}}{K_{I,H} + S_{[H],Opt}}} \quad \text{(Eq. 3)}$$

The kinetic expressions of the processes make it necessary to calculate the chemical equilibrium to obtain the concentration of given inorganic soluble components under its different species (CO_2, H_2S, NH_3). For this, acid-base and ion-pairing reactions are included in the model as equilibrium governed processes. This equilibrium is described by a set of non-linear algebraic equations including one law of mass action for each specie formed in each equilibrium system (Eq. 4) and one mass balance for each component (Eq. 5). Instead of using the charge balance for pH calculations, the model considers a mass-balance for the proton component (i.e. total proton is a model component). The software MINTEQA2 (Allison et al., 1991) was used for equilibrium and pH calculations. The mathematical formulation of MINTEQA2 can be summarized as follows (see MINTEQA2 user's manual version 4.03):

A system of *n* independent components that can be combined to form *m* species is represented by a set of mass action expressions in the form of:

$$x_i = K_i \prod_{j=1}^{N_c} x_j^{a_{ij}} \quad i = 1, 2, \ldots N_{sp} \quad \text{(Eq. 4)}$$

where x_i is the activity of the *i*th specie, x_j is the activity of the *j*th specie, a_{ij} is the stoichiometric coefficient of the *j*th component in the *i*th specie (see e-supplementary material: Table S4), K_i is the stability constant of the *i*th specie corrected for temperature variations with van't Hoff equation, N_{sp} is the number of species considered, and N_c is the number of components.

In addition to the mass action expression, the set of *n* independent components can be represented by *n* mass balance equations in the form of:

$$T_j = \sum_{i=1}^{N_{sp}} a_{ij} C_i \quad j = 1, 2, \ldots N_c \quad \text{(Eq. 5)}$$

where T_j is the total concentration of component j calculated in the kinetic model and C_i is the concentration of the *i*th specie. Equilibrium conditions are assumed.

The activity and concentration of every component or species are related through the corresponding activity coefficient, which depends on the ionic strength (Davies' equation):

$$x_i = \gamma_i C_i \quad i = 1, 2, \ldots N_{sp} \qquad \text{(Eq. 6)}$$

where γ_i is the activity coefficient for the *i*th species.

Equation 5 shows an example of the mass balance equations for the component NH_4^+:

$$S_{NH_X} = S_{NH_4^+} + S_{NH_3} \qquad \text{(Eq. 7)}$$

For more information on equilibrium, pH calculation and simulation procedure, see Serralta et al. (2004).

The BNRM2 collection model including SRB-related processes was implemented on DESASS software (Ferrer et al., 2008), which allows the user two possibilities for SRT control: i) to establish the SRT, or ii) to establish the sludge waste flow rate. In the first case (used for steady-state simulations) the software calculates the sludge waste flow rate required to maintain a selected SRT taking into account the suspended solids concentration. In the second case (for dynamic simulations), the software calculates the SRT value. The software can also set the retention capacity of the membrane to simulate different filtration technologies (e.g., microfiltration and ultrafiltration). In this work, ultrafiltration was used, thus complete retention of particulate compounds was considered. The model can be linked to a previously developed filtration model applied to AnMBR technology (Robles et al. 2013b) through the state variable X_{TSS}.

3.6. Model calibration

The AnMBR plant was continuously run under different operating conditions for 2.5 years to provide model development, calibration and validation. On-line calibration was carried out using the pseudo-

steady state conditions reached at the end of periods IX and XII. The parameters calibrated by this method were: maximum growth rates, decay rates, temperature coefficients, half saturation constants for substrate and electron acceptor, biomass yields and parameters related to the hydrolysis process. Half saturation constants for nutrients and inhibition constants were obtained from the literature. The main drawback of on-line calibration is that system dynamics can be reproduced by different sets of parameter values, so that off-line lab experiments were also conducted to calibrate the main heterotrophic SRB parameters by isolating specific heterotrophic SRB-related processes, mainly based on Sulfate Reduction Rate (SRR) measurements. These experiments provided information on the maximum SRB activity under certain conditions, including: biomass concentration, substrate and inhibitor concentrations, and operating temperature. Different experiments were carried out at different temperatures using different initial substrate and sulfate concentrations to determine the yield of heterotrophic SRB, the sulfate half-saturation constant, and the acetate and propionate half-saturation constants. The temperature was controlled by a thermostated water bath. During these experiments the time evolution of sulfate and VFA concentrations was measured. Since sulfide is oxidized to sulfate during the analytical procedure, sulfide was precipitated to obtain accurate sulfate concentration measurements.

The constrained Rosenbrock optimization method was applied to obtain the parameter values that were dynamically determined (on-line calibration). The AnMBR plant was simulated in an iterative process aimed at minimizing the sum of square relative errors. The variables used for the optimization were: soluble and total COD, sulfate and sulfide effluent concentrations, total and volatile suspended solids in the AnMBR, alkalinity, biogas flow rate and biogas composition (%CH4). The simulations started with initial model parameter values from the literature and were modified in successive simulations according to the results obtained within the previously established range and stopped when the set precision was reached. The tolerance criterion was set to 0.001 for each variable and the maximum number of iterations was set to 1500 for the optimization method. The model parameter values obtained were used for validating the model under steady-state and dynamic conditions.

The mass transfer coefficient for dissolved methane ($K_L a)_{CH4}$) was obtained by establishing the dissolved methane concentration as the 102% of the saturation concentration. When used to minimize membrane fouling, gas sparging avoids methane supersaturation. According to Merkel and Krauth (1999) the mass transfer coefficient for the rest of the gaseous species can be calculated from the methane coefficient using Eq (6)

$$K_L a)_i = K_L a)_{CH4} \cdot \sqrt{\frac{D_i}{D_{CH4}}} \quad \text{(Eq. 8)}$$

where $K_L a)_i$ is the mass-transfer coefficient of the gas i (d^{-1}); D_i is the diffusivity of the gas i.

3.7. Model validation

Five operating periods were selected for model validation under dynamic conditions: periods II, VI, IX, X, and XII, covering a wide range of the main operational parameters (SRT varied between 20 and 70 days, temperature between 20 and 33 ºC and HRT between 12 and 30 hours). The pseudo-steady state conditions reached at the end of these periods were used to validate the steady-state model. These periods were simulated to verify that both the model and the calibrated parameters were able to reproduce the plant behavior in operating conditions other than those used for mathematical fitting.

4. Results and discussion

4.1. Parameter calibration

Table 2 collects the stoichiometric and kinetic parameters resulting from the model calibration. It should be noted that the parameters related to SRB obtained a higher value for biomass yield than that obtained for the other bacterial groups, also the significant difference between the half saturation constant for acetate (5.12 mg COD·L^{-1}) and propionate (29.4 mg COD·L^{-1}). The high biomass yield was due to the external electron acceptor used by SRB, which leads SRB to outcompete methanogenic bacteria. The low propionate concentrations usually present in the AnMBR systems lead to acetogenic bacteria

outcompeting heterotrophic SRB because of the significant difference between half saturation constants for both bacterial groups (2.2 mg COD·L^{-1} for X_{PRO} and 29.4 mg COD·L^{-1} for X_{ASRO}).

4.2. Steady-state model performance

Table 3 shows the results of the simulation of the pseudo-steady state conditions reached at the end of periods VI, IX, X and XII. The comparison of the modeled and experimental data for the main characteristics of permeate, waste sludge and biogas showed that the model was able to reproduce the AnMBR performance in different steady-state conditions.

4.3. Dynamic model performance

To validate the model behavior in dynamic conditions, five operating periods conducted at different SRTs (70, 40, 30, 40 and 20 days) were simulated (periods II, VI, IX, X and XII, respectively). In these periods, the main operational parameters were modified (SRT from 70 d to 40 d in period VI, and from 30 d to 40 d in period X; temperature from 15ºC to 20ºC in period IX and from 20ºC to 30ºC in period XI and HRT from 17 h to 11 h in period II, and from 15 h to 40h in period XI). Figures 3 to 5 show the experimental results obtained in the AnMBR plant (dashed lines) compared to the model predictions (continuous lines). Additional periods are provided as e-supplementary material (Figure S1 and Figure S2).

Figure 3 shows the simulation results for period II. During this period, operating temperature and SRT remained virtually constant, while the HRT was gradually reduced from 17 to 11 hours. As Figure 3a shows, TS and VS increased in the mixed liquor due to the reduced HRT. From day 70 to 80 approx., there were peaks in OLR (see COD/SO_4^{2-}-S ratio in Figure 3g), which were reflected in the accumulation of VFA and ammonium (see Figure 3c and Figure 3d, respectively). Figure 3g also shows that the organic peak loads promoted the growth of both acidogenic (X_{AO}) and acetogenic (X_{PRO}) organisms. The increased fermentation produced more hydrogen, which was completely consumed by the autotrophic SRB (X_{ASRO}), as shown by the absence of hydrogenotrophic methanogens (X_{HMO}). These results are in

agreement with the expected trend, since X_{ASRO} gain more energy from hydrogen consumption and have higher substrate affinity, maximum growth rate and biomass yield than X_{HMO} (see Table 2). Conversely, organic peak loads resulted in a decrease of heterotrophic SRB (X_{HSRO}) concentration, since more sulfate was consumed by X_{ASRO}. The higher availability of acetate derived from the COD/SO_4^{2-}-S peaks and the reduced X_{HSRO} thus increased acetoclastic methanogen (X_{AMO}) concentration.

Figure 4 gives the simulation results for period VI. At the beginning of this period, SRT was reduced from 70 to 40 days. Mixed liquor VS and TS gradually dropped due to the increase in the waste sludge associated with the lower SRT (see Figure 3a). The lower SRT and organic loading rate (HRT was increased from 24 h to 34 h) led to a reduced concentration of most of the bacterial groups, SRB being one of the most affected heterotrophics (see Figure 4g). It is Important to note the behavior between days 470 and 490, when high sulfate and low sulfide effluent concentrations were observed (see Figure 4e) as a consequence of the low influent organic load, which restricted sulfate-reducing processes. The sulfide produced was distributed among its different species, depending on the pH. According to Lens et al. (1998), only the first dissociation equilibrium of H_2S is of important at neutral pH, so that most of the sulfide produced was present either as the undissociated form (H_2S) or the ionic species HS^-, the concentration of S^{2-} being negligible. The undissociated form is presumably responsible for the inhibitory effect of sulfide, since only uncharged molecules can permeate the cell membrane (Maree and Strydom, 1985). For instance, for the operating temperature of period VI, the pKa of the first dissociation equilibrium of H_2S is around 6.9 (Lens et al. 1998), indicating that only the undissociated form H_2S and the ionic species HS^- concentrations were significant. Specifically, the AnMBR pH during this period was around 6.9, resulting in H_2S concentrations around 80% of the total sulfide produced. Fedorovich et al. (2003) reported 50% inhibitory values of H_2S ($K_{I,[H2S]}$) for several microbial groups considering first order inhibition kinetics (see Table 2). The most sensitive groups to H_2S inhibition were hydrogenotrophic and acetotrophic methanogens ($X_{HMO}$and X_{ACO}, respectively), whose activity was half inhibited at H_2S concentrations of 213 and 245 mg H_2S-S·L^{-1}. Sulfate reducer activity was half inhibited at H_2S

concentrations of 265 mg H_2S-S·L^{-1}. SRO and methanogenic activity was thus slightly inhibited during the experimental period.

Figure 5 shows the simulation results for period X, during which SRT was raised from 30 to 40 days while ambient temperature remained around 20 ºC, which increased solids concentration in the mixed liquor (see Figure 5a).Sulfate was not completely consumed by the SRB at the beginning of period X (see Figure 5e). During this period, sulfate concentration rose to 139 mg SO_4^{2-}-S·L^{-1}, while the average influent value was 108 mg SO_4^{2-}-S·L^{-1}. The extra sulfate load in the system intensified the competition between SRB and methanogens for the available substrates as a result of the reduced COD/SO_4^{2-}-S ratio. Initially, the existing SRB population was not able to completely consume the available sulfate. However, they gradually outcompeted the methanogens, as shown by the shrinking biogas production and the rising X_{ASRO} (see Figure 5b and Figure 5g, respectively). This increase in influent sulfate concentration affected methane production, and the influent flow was doubled between days 675 and 685, thus affecting both the loading rate entering the system and the extraction of compounds such as dissolved methane due to a significant decrease in the HRT. The higher COD/SO_4^{2-}-S ratio between days 674 and 694 promoted the growth of X_{AO}, X_{PRO}, X_{ASRO} and reduced the concentration of X_{HSRO}. As in period II, the availability of acetate stimulated the growth of X_{ACO}.

Sub-plot g in Figures 3 to 5 shows the population dynamics predicted by the model. Autotrophic sulfate reducers (X_{ASRO}) outcompeted hydrogenotrophic methanogens (X_{HMO}) since, according to process fundamentals, X_{ASRO} gain more energy from hydrogen consumption, and have higher substrate affinity, growth rate and cell yield than X_{HMO} (Lens et al., 1998). Indeed, X_{HMO} concentration was negligible during the whole experimental period and the electrons from the hydrogen produced were derived to sulfide rather than to methane, proportionally reducing the UWW methane potential. Sulfate was consumed preferentially by X_{ASRO} as long as hydrogen and sulfate were present. This is in agreement with the findings by Laanbroek et al. (1984), who reported autotrophic SRB *Desulfovibrio spp* having a higher

affinity for the substrates than other heterotrophic SRB *(Desulfobulbus spp and Desulfobacter spp*) under sulfate-limited environments. This is the reason why the concentration of heterotrophic sulfate reducers (X_{HSRO}) was inversely affected by the organic loading rate, which enhanced hydrogen production via fermentation. X_{HSRO} can metabolize a wide range of substrates and competed for the common substrates with acetogens (X_{PRO}) and acetoclastic methanogens (X_{ACO}) as long as sulfate was left from the autotrophic sulfate reduction. The concentration of X_{PRO} remained virtually steady during each period, indicating that X_{PRO} successfully competed with X_{HSRO}. Conversely, in spite of the residual acetate-derived methane production, a decreasing trend was detected for X_{ACO} when sulfate was not limited (low organic load episodes during summer periods VI and XII). In any case, X_{HSRO} were sulfate-limited most of the time and it was completely reduced as long as the BOD:SO_4^{2-}-S ratio was above the stoichiometric threshold (2 g BOD g^{-1} S). Under sulfate-limited conditions, acetate electrons were also derived towards sulfide rather than to methane, reducing the UWW methane potential. A lower methane potential entails a loss of energy efficiency for the system, since less energy can be recovered either as power or heat.

4.4. Overall model performance

The results of the model validation for all the variables evaluated throughout all the operating periods gave an overall R^2 coefficient of 0.9966 (see e-supplementary material: Figure S3, which represents a scatter plot of the simulated values versus the experimental data). The graph includes more than 1000 pairs of data, showing the reproducibility of the model and the parameters fitted from experimental data collected from the pilot plant. Besides the operating dynamics (SRT, HRT and T) and influent characterization, the model was able to accurately reproduce the process performance. It should be noted that the model reproduced the solids concentration dynamics in the mixed liquor, which is essential in AnMBRs due to the need to integrate both biochemical and filtration models. The AD sub-model was coupled to a filtration model through the mixed liquor TS concentration, also developed, calibrated and validated with the data from the AnMBR plant. Further details of the filtration model and the integration with the biochemical model can be found in Robles et al. (2014, 2013b, 2013a).

The model also faithfully reproduced the dynamics of both alkalinity and pH in the mixed liquor. Besides chemical precipitation also affecting membrane scaling, alkalinity and pH affect species equilibrium and gas-liquid transfer processes. In this respect, it is vital to minimize oversaturation of dissolved gases in the liquid phase, which can be achieved by adequate reactor stirring optimization. As pH also plays a key role in the equilibrium of other dissolved gases (e.g. NH_3, H_2S) between liquid and gas phases, thus affecting the quality of the biogas produced, accurate modeling of dissolved gas concentration and pH is needed to evaluate and optimize AnMBR feasibility for UWW treatment at ambient temperatures.

The simulation data satisfactorily represented experimental data related to SRB processes, which have a significant impact on the performance of the AnMBR fed with sulfate-rich UWW. Results from other compounds such as VFA and methane production also accurately reproduced the interactions between SRB and methanogens, with a lower complexity level than other available models. It was also able to capture the reduced biogas production from SRB/methanogens competition during low COD/SO_4^{2-}-S ratio events (see Figure 5b). The model's population shift predictions showed that acidogenic bacteria concentrations were mainly dependent on the system's organic loading rate, whose trend was accurately described by the COD/SO_4^{2-}-S ratio, and the temperature, which strongly affects the hydrolysis rate. Since hydrogen was mainly produced during fermentation, the concentration of autotrophic SRB followed the same trend. The higher the concentration of X_{ASRO}, the higher the sulfate reduced autotrophically and the lower the X_{HSRO} concentration. All the methane production was due to acetoclastic methanogens, since hydrogenotropic methanogens were outcompeted by autrotropihc SRB.

It should be noted that the model could require a widened structure depending, for instance, on the substrate degradation complexity or the objective of the modeling task. In this respect, Ahmed and Rodríguez (2018) also stated that complex model structures are only recommended for specific experimental cases. These authors evaluated the complexity of five ADM1-based model structures differing in the number of SRB groups considered and based on the electron donors used. Their objective was to evaluate the accuracy of each modeling approach for different aims, thus helping developers and

users to decide on the appropriate degree of complexity required. The results found that it is possible to simulate the AD of cane molasses with high COD and high sulfate feed, even when only acetate-utilizing and hydrogen-utilizing SRB are considered, achieving a good performance/complexity balance in terms of prediction errors against experimental data.

Determining the biological complexity for the modeling goal (particularly the inclusion of alternative electron sinks) is thus a key issue, while a benchmark modeling framework including standardized calibration protocols could be needed to deal with possible microbial ecology shifts affecting model accuracy.

4.5. Implications for AnMBR implementation

As already mentioned, modeling sulfate-reducing processes is a vital part of evaluating the feasibility of AnMBR for UWW treatment because of different factors.

Modeling the amount of methane produced facilitates the design and selection of suitable approaches for dissolved methane capture or removal. For the former, degasification by non-porous membranes and micro-porous membrane contactors are promising technologies for dissolved methane recovery. Some authors have reported net energy recoveries when capturing the methane dissolved in AnMBR effluents through membrane processes (Cookney et al., 2016; Henares et al., 2017), while others obtained high nitrogen removal rates when using dissolved methane as the electron donor for denitrification in a post-treatment process (Sánchez-Ramírez et al. 2015; Pelaz et al. 2018).

Concerning corrosion issues, AnMBR biogas contains variable amounts of H_2S, which can affect all biogas conversions and equipment. The H_2S concentration in the biogas was much higher than in conventional AD, likely due to the much lower COD/SO_4^{2-}-S ratio in the UWW than in other AD substrates (e.g. sewage sludge). The H_2S content in the AnMBR biogas ranged from around 10000 to 25000 ppm,

which were adequately reproduced by the model. As the quality requirements depend on the use the biogas is to be put to, acid-biogas “sweetening” could be required, according to the H_2S tolerance of the CHP technology used, before it can be energetically valorized, since H_2S is transformed into highly corrosive sulfuric acid on combustion.

A post-treatment step could be required for effluent nutrient removal or recovery, depending on the characteristics of the receiving water body. It could also be necessary to remove sulfide, since it can be detrimental to downstream processes. Sulfide contributes to the effluent COD, which has discharge limits in most countries. Last, but not least, recovery of dissolved methane, which is an energy carrier with high global warming potential, could help to reduce GHG emissions while enhancing the system’s energy recovery potential, which means it is essential to accurately reproduce effluent quality for designing classical or advanced techniques for nutrient, sulfide or dissolved methane removal or recovery. For instance, the high-quality nutrient-loaded permeate produced makes it suitable for fertigation. Nevertheless, when fertigation is limited by regulations, a combination of AnMBR with a nutrient recovery post-treatment method can be used, e.g. membrane contactors, ion exchange, or photosynthetic bioreactors. Most of these systems require solid- and sulfide-free influents with low organic contents, so that modeling effluent quality in terms of VFA and other organics or sulfide is needed to evaluate the technical, economic and environmental feasibility of combining AnMBR with selected post-treatments. Since a single optimal technological solution for the whole range of situations has yet to be proposed, modeling nutrient, sulfide and dissolved methane effluent quality would help to evaluate not only the technical feasibility of the solution but also different environmental impact indexes, such as prevention of eutrophication in aquatic environments, reduction of the environmental impact of phosphate mining, or reducing the energy demand for chemical fertilizer production. Plant-wide modeling would also assist in the selection of optimized layouts for resource recovery and removal, such as combining AnMBR with an AS-based post-treatment for nutrient removal, or AnMBR with classical and emerging technologies for nutrient recovery (see e.g. Robles et al., 2020).

5. Conclusions

The extended BNRM2S model successfully reproduced the performance of an AnMBR pilot plant that treated sulfate-rich UWW under different conditions. Despite the operating dynamics (SRT, HRT and T) and influent composition, the model was able to reproduce the process performance and successfully captured influent loading rate dynamics and effluent quality, which is essential for designing classical or advanced nutrient removal or recovery techniques. High-sulfate and low-sulfide effluent concentrations were also reproduced at lower influent BOD:SO_4^{2-}-S ratios. In this respect, modeling the competition between SRB and methanogens, which affect methane production, facilitates the design and selection of suitable approaches for dissolved methane capture or removal. The proposed model can thus be used for different purposes: designing and upgrading AnMBR and other anaerobic systems, evaluating process performance in different situations or developing control strategies to optimize process performance.

ACKNOWLEDGEMENTS

This research work was supported by the Spanish Ministry of Economy and Competitiveness [Grants CTM2011-28595-C02-01/02, CTM2017-86751-C2-1-R and CTM2017-86751-C2-2-R]; Co-funded by the European Regional Development Fund [Grant CTM2011-28595-C02-01/02].

REFERENCES

Ahammad, S.Z., Gomes, J., Sreekrishnan, T.R., 2011. A Mathematical Model for the Interactive Behavior of Sulfate-Reducing Bacteria and Methanogens During Anaerobic Digestion. Water Environ. Res. 83, 791–801. https://doi.org/10.2175/106143011X12989211840819

Ahmed, W., Rodríguez, J., 2018. Modelling sulfate reduction in anaerobic digestion: Complexity evaluation and parameter calibration. Water Res. 130, 255–262. https://doi.org/10.1016/j.watres.2017.11.064

Ahmed, W., Rodríguez, J., 2017. Generalized parameter estimation and calibration for biokinetic models using correlation and single variable optimisations: Application to sulfate reduction modelling in anaerobic digestion. Water Res. 122, 407–418. https://doi.org/10.1016/J.WATRES.2017.05.067

Allison J. D., Brown D. S. y Novo-Gradac K. J. (1991) MINTEQA2/ PRODEFA2, A Geochemical Assessment Model for Environmental Systems: Version 3.0. EPA/600/3-91/021, USEPA, Washington, D.C.

APHA, 2005. Standard Methods for the Examination of Water and Wastewater. American Public Health Association, Washington, DC.

Anaerobic Digestion & Bioresources Association, 2013. The practical guide to Anaerobic Digestion [WWW Document]. Prod. using biogas. URL http://adbioresources.org/wp-content/uploads/2013/06/59-80_chapter5_v41.pdf

Aquino, S.F., Stuckey, D.C., 2008. Integrated model of the production of soluble microbial products (SMP) and extracellular polymeric substances (EPS) in anaerobic chemostats during transient conditions. Biochem. Eng. J. 38, 138–146. https://doi.org/10.1016/j.bej.2007.06.010

Barat, R., Serralta, J., Ruano, M. V, Jiménez, E., Ribes, J., Seco, A., Ferrer, J., 2013. Biological Nutrient Removal Model No. 2 (BNRM2): a general model for wastewater treatment plants. Water Sci. Technol. 67, 1481–1489.

Barrera, E.L., Spanjers, H., Solon, K., Amerlinck, Y., Nopens, I., Dewulf, J., 2015. Modeling the anaerobic digestion of cane-molasses vinasse: Extension of the Anaerobic Digestion Model No. 1 (ADM1) with sulfate reduction for a very high strength and sulfate rich wastewater. Water Res. 71, 42–54. https://doi.org/10.1016/J.WATRES.2014.12.026

Batstone, D.J., 2006. Mathematical modelling of anaerobic reactors treating domestic wastewater: Rational criteria for model use. Rev. Environ. Sci. Biotechnol. https://doi.org/10.1007/s11157-005-7191-z

Batstone, D.J., Keller, J., Angelidaki, I., Kalyuzhnyi, S. V., Pavlostathis, S.G., Rozzi, A., Sanders, W.T.M., Siegrist, H., Vavilin, V.A., 2002. The IWA Anaerobic Digestion Model No 1 (ADM1).

Water Sci. Technol. 45, 65–73. https://doi.org/10.2166/wst.2008.678

Batstone, D.J., Keller, J., Steyer, J.P., 2006. A review of ADM1 extensions, applications, and analysis: 2002-2005. WATER Sci. Technol. 54, 1–10. https://doi.org/10.2166/wst.2006.520

Batstone, D.J., Puyol, D., Flores-Alsina, X., Rodríguez, J., 2015. Mathematical modelling of anaerobic digestion processes: applications and future needs. Rev. Environ. Sci. Bio/Technology. https://doi.org/10.1007/s11157-015-9376-4

Becker, A.M., Yu, K., Stadler, L.B., Smith, A.L., 2017. Co-management of domestic wastewater and food waste: A life cycle comparison of alternative food waste diversion strategies. Bioresour. Technol. 223, 131–140. https://doi.org/10.1016/j.biortech.2016.10.031

Benyahia, B., Sari, T., Cherki, B., Harmand, J., 2013. Anaerobic membrane bioreactor modeling in the presence of Soluble Microbial Products (SMP) - the Anaerobic Model AM2b. Chem. Eng. J. 228, 1011–1022. https://doi.org/10.1016/j.cej.2013.05.073

Bernard, O., Hadj-Sadok, Z., Dochain, D., Genovesi, A., Steyer, J.P., 2001. Dynamical model development and parameter identification for an anaerobic wastewater treatment process. Biotechnol. Bioeng. 75, 424–438. https://doi.org/10.1002/bit.10036

Cassidy, J., Lubberding, H.J., Esposito, G., Keesman, K.J., Lens, P.N.L., 2015. Automated biological sulphate reduction: A review on mathematical models, monitoring and bioprocess control. FEMS Microbiol. Rev. 39, 823–853. https://doi.org/10.1093/femsre/fuv033

Charfi A., Thongmak, N., Benyahia B., Aslam M., Harmand J., Amar N. B., Lesage G., Sridang P., Kim J., Heran M., 2017. A modelling approach to study the fouling of an anaerobic membranebioreactor for industrial wastewater treatment. Bioresour. Technol.245, 207-215

Chen, C., 2020. Anaerobic membrane bioreactors for sustainable and energy-efficient municipal wastewater treatment, in: Current Developments in Biotechnology and Bioengineering. pp. 335–366. https://doi.org/10.1016/B978-0-12-819852-0.00014-2

Cookney, J., Mcleod, A., Mathioudakis, V., Ncube, P., Soares, A., Jefferson, B., McAdam, E.J., 2016. Dissolved methane recovery from anaerobic effluents using hollow fibre membrane contactors. J.

Memb. Sci. https://doi.org/10.1016/j.memsci.2015.12.037

Copp, J.B., Belia, E., Snowling, S., Schraa, O., 2005. Anaerobic digestion: a new model for plant-wide wastewater treatment process modelling. Water Sci. Technol. 52, 1–11.

Corominas, L., Rieger, L., Takáks, I., Ekama, G., Hauduc, H., Vanrolleghem, P.A., Oehmen, A., Gernaey, K. V, Loosdrecht, M.C.M. Van, Comeau, Y., 2010. New framework for standardized notation in wastewater treatment modelling 841–857. https://doi.org/10.2166/wst.2010.912

Crone, B.C., Garland, J.L., Sorial, G.A., Vane, L.M., 2016. Significance of dissolved methane in effluents of anaerobically treated low strength wastewater and potential for recovery as an energy product: A review. Water Res. https://doi.org/10.1016/j.watres.2016.08.019

Donoso-bravo, A., Mailier, J., Martin, C., Rodrı, J., Aceves-lara, A., Vande, A., 2011. Model selection, identification and validation in anaerobic digestion: A review. https://doi.org/10.1016/j.watres.2011.08.059

Fedorovich, V., Lens, P., Kalyuzhnyi, S., 2003. Extension of Anaerobic Digestion Model No. 1 with Processes of Sulfate Reduction. Appl. Biochem. Biotechnol. 109, 33–46. https://doi.org/10.1385/ABAB:109:1-3:33

Fernández-Arévalo, T., Lizarralde, I., Fdz-Polanco, F., Pérez-Elvira, S.I., Garrido, J.M., Puig, S., Poch, M., Grau, P., Ayesa, E., 2017. Quantitative assessment of energy and resource recovery in wastewater treatment plants based on plant-wide simulations. Water Res. 118, 272–288. https://doi.org/10.1016/j.watres.2017.04.001

Ferrer, J., Seco, A., Serralta, J., Ribes, J., Manga, J., Asensi, E., Morenilla, J.J., Llavador, F., 2008. DESASS: A software tool for designing, simulating and optimising WWTPs. Environ. Model. Softw. 23. https://doi.org/10.1016/j.envsoft.2007.04.005

Fomichev, A.O., Vavilin, V.A., 1997. The reduced model of self-oscillating dynamics in an anaerobic system with sulfate-reduction. Ecol. Modell. 95, 133–144. https://doi.org/10.1016/S0304-3800(96)00041-5

Frunzo, L., Esposito, G., Pirozzi, F., Lens, P., 2012. Dynamic mathematical modeling of sulfate

reducing gas-lift reactors. Process Biochem. 47, 2172–2181. https://doi.org/10.1016/J.PROCBIO.2012.08.010

Giménez, J. B., Carretero, L., Gatti, M.N., Martí, N., Borrás, L., Ribes, J., Seco, A., 2012a. Reliable method for assessing the COD mass balance of a submerged anaerobic membrane bioreactor (SAMBR) treating sulphate-rich municipal wastewater. Water Sci. Technol. 66, 494–502. https://doi.org/10.2166/wst.2012.184

Giménez, J. B., Martí, N., Ferrer, J., Seco, A., 2012b. Methane recovery efficiency in a submerged anaerobic membrane bioreactor (SAnMBR) treating sulphate-rich urban wastewater: Evaluation of methane losses with the effluent. Bioresour. Technol. 118, 67–72. https://doi.org/10.1016/j.biortech.2012.05.019

Giménez, J.B., Martí, N., Robles, A., Ferrer, J., Seco, A., 2014. Anaerobic treatment of urban wastewater in membrane bioreactors: Evaluation of seasonal temperature variations. Water Sci. Technol. 69. https://doi.org/10.2166/wst.2014.069

Giménez, J.B., Robles, A., Carretero, L., Durán, F., Ruano, M.V., Gatti, M.N., Ribes, J., Ferrer, J., Seco, A., 2011. Experimental study of the anaerobic urban wastewater treatment in a submerged hollow-fibre membrane bioreactor at pilot scale. Bioresour. Technol. 102. https://doi.org/10.1016/j.biortech.2011.07.014

Guo, W., Ngo, H.H., Chen, C., Pandey, A., 2016. Anaerobic Membrane Bioreactors for Future Green Bioprocesses, in: Green Technologies for Sustainable Water Management. American Society of Civil Engineers, pp. 867–901. https://doi.org/https://doi.org/10.1061/9780784414422.ch25

Harerimana, C., Keffala, C., Jupsin, H., Vasel, J.-L., 2013. Development of a simple model for anaerobic digestion based on preliminary measurements of the bacterial sulphur activity in wastewater stabilization ponds. Environ. Technol. 34, 2213–2220. https://doi.org/10.1080/09593330.2012.725773

Henares, M., Izquierdo, M., Marzal, P., Martínez-Soria, V., 2017. Demethanization of aqueous anaerobic effluents using a polydimethylsiloxane membrane module: Mass transfer, fouling and energy analysis. Sep. Purif. Technol. 186, 10–19. https://doi.org/10.1016/j.seppur.2017.05.035

Kadam, R., Panwar, N.L., 2017. Recent advancement in biogas enrichment and its applications. Renew. Sustain. Energy Rev. 73, 892–903. https://doi.org/10.1016/j.rser.2017.01.167

Kalyuzhnyi, S.V., Fedorovich, V.V., 1998. Mathematical modelling of competition between sulphate reduction and methanogenesis in anaerobic reactors. Bioresour. Technol. 65, 227–242. https://doi.org/10.1016/S0960-8524(98)00019-4

Knobel, A.N., Lewis, A.E., 2002. A mathematical model of a high sulphate wastewater anaerobic treatment system. Water Res. 36, 257–265. https://doi.org/10.1016/S0043-1354(01)00209-3

Kythreotou, N., Florides, G., Tassou, S.A., 2014. A review of simple to scientific models for anaerobic digestion. Renew. Energy 71, 701–714. https://doi.org/10.1016/J.RENENE.2014.05.055

Laanbroek, H.J., Geerlings, H.J., Sijtsma, L., Veldkamp, H., 1984. Competition for sulfate and ethanol among Desulfobacter, Desulfobulbus, and Desulfovibrio species isolated from intertidal sediments. Applied Environmental Microbiology 47, 329-334.

Lei, Z., Yang, S., Li, Y. you, Wen, W., Wang, X.C., Chen, R., 2018. Application of anaerobic membrane bioreactors to municipal wastewater treatment at ambient temperature: A review of achievements, challenges, and perspectives. Bioresour. Technol. 267, 756–768. https://doi.org/10.1016/j.biortech.2018.07.050

Lens, P.N.L., Visser, A., Janssen, A.J.H., Pol, L.W.H., Lettinga, G., 1998. Biotechnological Treatment of Sulfate-Rich Wastewaters. Crit. Rev. Environ. Sci. Technol. 28, 41–88. https://doi.org/10.1080/10643389891254160

Lizarralde, I., Fernández-Arévalo, T., Manas, A., Ayesa, E., Grau, P., 2019. Model-based opti mization of phosphorus management strategies I n Sur WWTP, Madrid. Water Res. 153, 39–52. https://doi.org/10.1016/J.WATRES.2018.12.056

Maaz, M., Yasin, M., Aslam, M., Kumar, G., Atabani, A.E., Idrees, M., Anjum, F., Jamil, F., Ahmad, R., Khan, A.L., Lesage, G., Heran, M., Kim, J., 2019. Anaerobic membrane bioreactors for wastewater treatment: Novel configurations, fouling control and energy considerations. Bioresour. Technol. 283, 358–372. https://doi.org/10.1016/j.biortech.2019.03.061

Maree, J.P., Strydom, W.F., 1985. Biological sulphate removal in an upflow packed bed reactor.Water Res. 19, 1101–1106. https://doi.org/https://doi.org/10.1016/0043-1354(85)90346-X

Martí, N., Barat, R., Seco, A., Pastor, L., Bouzas, A., 2017. Sludge management modeling to enhance P-recovery as struvite in wastewater treatment plants. J. Environ. Manage. 196, 340–346. https://doi.org/10.1016/J.JENVMAN.2016.12.074

Mei, X., Wang, Z., Miao, Y., Wu, Z., 2016. Recover energy from domestic wastewater using anaerobic membrane bioreactor: Operating parameters optimization and energy balance analysis. Energy 98, 146–154. https://doi.org/10.1016/j.energy.2016.01.011

Merkel, W., Krauth, K., 1999. Mass transfer of carbon dioxide in anaerobic reactors under dynamic substrate loading conditions. Water Res. https://doi.org/10.1016/S0043-1354(98)00434-5

Moosbrugger, R.E., Wentzel, M.C., Ekama, G.A., Marais, G., 1992. Simple titration procedures to determine H2CO3* alkalinity and short-chain fatty acids in aqueous solutions. Pretoria.

Pelaz, L., Gómez, A., Garralón, G., Letona, A., Fdz-Polanco, M., 2018. Recirculation of gas emissions to achieve advanced denitrification of the effluent from the anaerobic treatment of domestic wastewater. Bioresour. Technol. 250, 758–763. https://doi.org/10.1016/j.biortech.2017.11.104

Pretel, R., Robles, A., Ruano, M.V., Seco, A., Ferrer, J., 2016. Economic and environmental sustainability of submerged anaerobic MBR-based (AnMBR-based) technology as compared to aerobic-based technologies for moderate-/high-loaded urban wastewater treatment. J. Environ. Manage. 166. https://doi.org/10.1016/j.jenvman.2015.10.004

Pretel, R., Robles, A., Ruano, M. V., Seco, A., Ferrer, J., 2014. The operating cost of an anaerobic membrane bioreactor (AnMBR) treating sulphate-rich urban wastewater. Sep. Purif. Technol. 126, 30–38. https://doi.org/10.1016/j.seppur.2014.02.013

Raskin, L., Skerlos, S., Love, N.G., Smith, A.L., 2012. Anaerobic Membrane Bioreactors for Sustainable Wastewater Treatment. https://doi.org/10.2166/9781780400532

Robles, Á., Aguado, D., Barat, R., Borrás, L., Bouzas, A., Bautista Giménez, J., Martí, N., Ribes, J., Victoria Ruano, M., Serralta, J., Ferrer, J., Seco, A., 2020. New frontiers from removal to recycling of

nitrogen and phosphorus from wastewater in the circula economy. Bioresour. Technol. 122673. https://doi.org/10.1016/J.BIORTECH.2019.122673

Robles, Á., Ruano, M.V., Charfi, A., Lesage, G., Heran, M., Harmand, J., Seco, A., Steyer, J.-P., Batstone, D.J., Kim, J., Ferrer, J., 2018. A review on anaerobic membrane bioreactors (AnMBRs) focused on modelling and control aspects. Bioresour. Technol. 270, 612–626. https://doi.org/https://doi.org/10.1016/j.biortech.2018.09.049

Robles, A., Ruano, M.V., Ribes, J., Seco, A., Ferrer, J., 2013a. Mathematical modelling of filtration in submerged anaerobic MBRs (SAnMBRs): Long-term validation. J. Memb. Sci. 446, 303–309. https://doi.org/10.1016/J.MEMSCI.2013.07.001

Robles, A., Ruano, M. V., Ribes, J., Seco, A., Ferrer, J., 2014. Global sensitivity analysis of a filtration model for submerged anaerobic membrane bioreactors (AnMBR). Bioresour. Technol. 158, 365–373. https://doi.org/10.1016/j.biortech.2014.02.087

Robles, A., Ruano, M. V., Ribes, J., Seco, A., Ferrer, J., 2013b. A filtration model applied to submerged anaerobic MBRs (SAnMBRs). J. Memb. Sci. 444, 139–147. https://doi.org/10.1016/j.memsci.2013.05.021

Sánchez-Ramírez, J.E., Seco, A., Ferrer, J., Bouzas, A., García-Usach, F., 2015. Treatment of a submerged anaerobic membrane bioreactor (SAnMBR) effluent by an activated sludge system: The role of sulphide and thiosulphate in the process. J. Environ. Manage. 147, 213–218. https://doi.org/10.1016/J.JENVMAN.2014.04.043

Sanchis-Perucho, P., Robles, Á., Durán, F., Ferrer, J., Seco, A., 2020. PDMS membranes for feasible recovery of dissolved methane from AnMBR effluents. J. Memb. Sci. 604, 118070. https://doi.org/https://doi.org/10.1016/j.memsci.2020.118070

Seco, A., Ribes, J., Serralta, J., Ferrer, J., 2004. Biological nutrient removal model No.1 (BNRM1). Water Sci. Technol. 50, 69–70. https://doi.org/10.2166/wst.2004.0361

Seco, A., Ruano, M. V, Ruiz-Martinez, A., Robles, A., Barat, R., Serralta, J., Ferrer, J., 2020. Plant-wide modelling in wastewater treatment: showcasing experiences using the Biological Nutrient

Removal Model. Water Sci. Technol. https://doi.org/10.2166/wst.2020.056

Serralta, J., Ferrer, J., Borrás, L., Seco, A., 2004. An extension of ASM2d including pH calculation. Water Res. 38, 4029–4038. https://doi.org/10.1016/J.WATRES.2004.07.009

Shin, C., Bae, J., 2018. Current status of the pilot-scale anaerobic membrane bioreactor treatments of domestic wastewaters: A critical review. Bioresour. Technol. 247, 1038–1046. https://doi.org/10.1016/j.biortech.2017.09.002 Solon, K., Volcke, E.I.P., Spérandio, M., Van Loosdrecht, M.C.M., 2019. Resource recovery and wastewater treatment modelling. Environ. Sci. Water Res. Technol. 5, 631–642. https://doi.org/10.1039/c8ew00765a

Weiland, P., 2010. Biogas production: Current state and perspectives. Appl. Microbiol. Biotechnol. 85, 849–860. https://doi.org/10.1007/s00253-009-2246-7

Widdel, F. 1988. Microbiology and ecology of sulphate and sulphur-reducing bacteria. In A. Zehnder, Biology of anaerobic microorganisms (pp. 469-585). New York: Wiley.

Ye, Y., Ngo, H.H., Guo, W., Chang, S.W., Nguyen, D.D., Zhang, X., Zhang, J., Liang, S., 2020. Nutrient recovery from wastewater: From technology to economy. Bioresour. Technol. Reports 100425. https://doi.org/10.1016/j.biteb.2020.100425

Zaher, U., Grau, P., Benedetti, L., Ayesa, E., Vanrolleghem, P.A., 2007. Transformers for interfacing anaerobic digestion models to pre- and post-treatment processes in a plant-wide modelling context. Environ. Model. Softw. 22, 40–58. https://doi.org/10.1016/J.ENVSOFT.2005.11.002

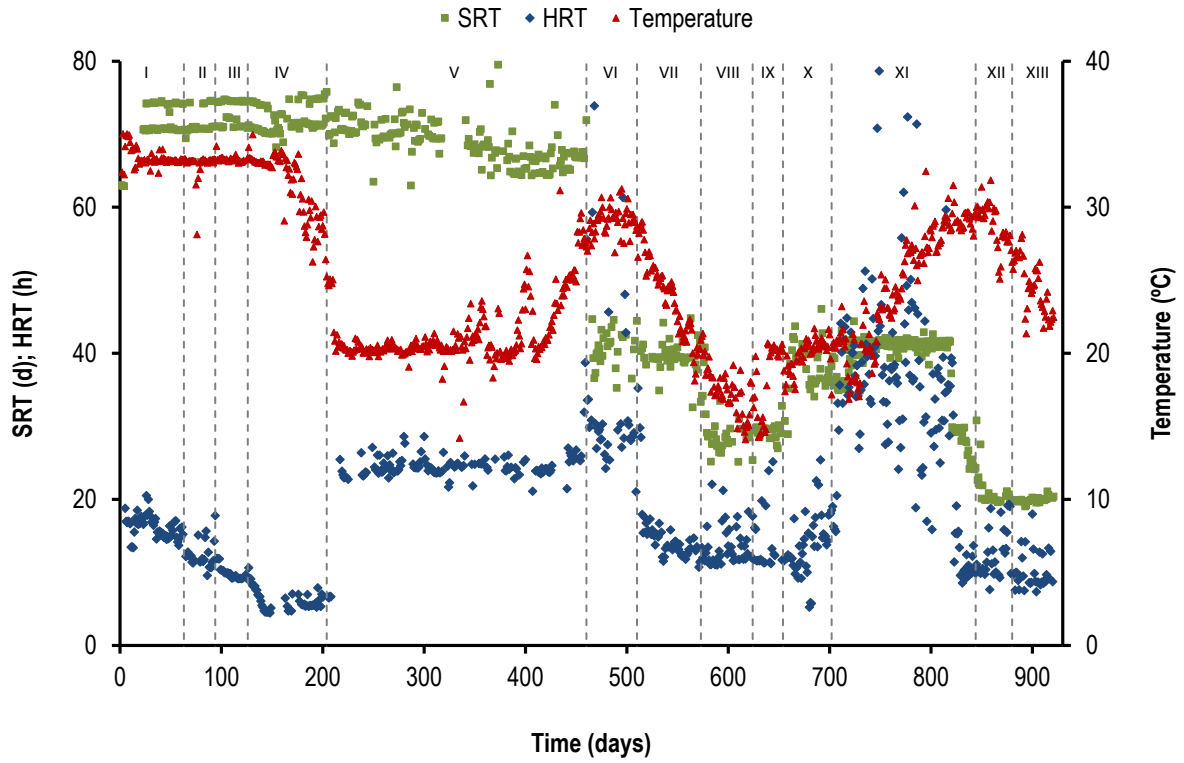

Figure 1. Evolution during the experimental period of daily average values for (a) sludge retention time (SRT), (b) hydraulic retention time (HRT), and mixed liquor temperature in the reactor.

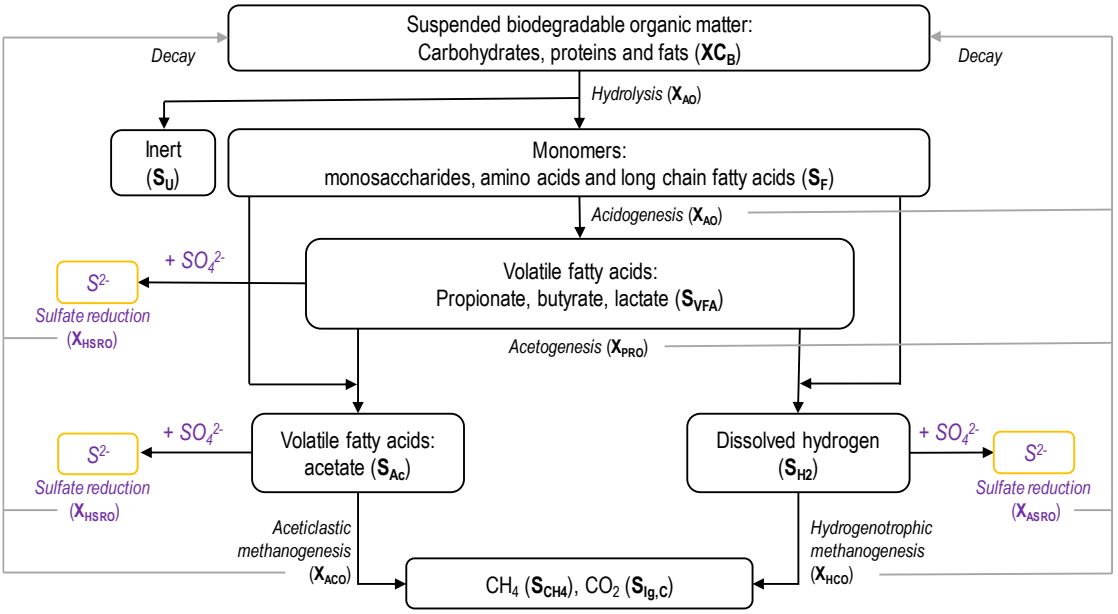

Figure 2. Schematic representation of the biochemical processes included in the anaerobic model extracted from the collection model BNRM2S and the additional processes for sulfate reducing modelling.

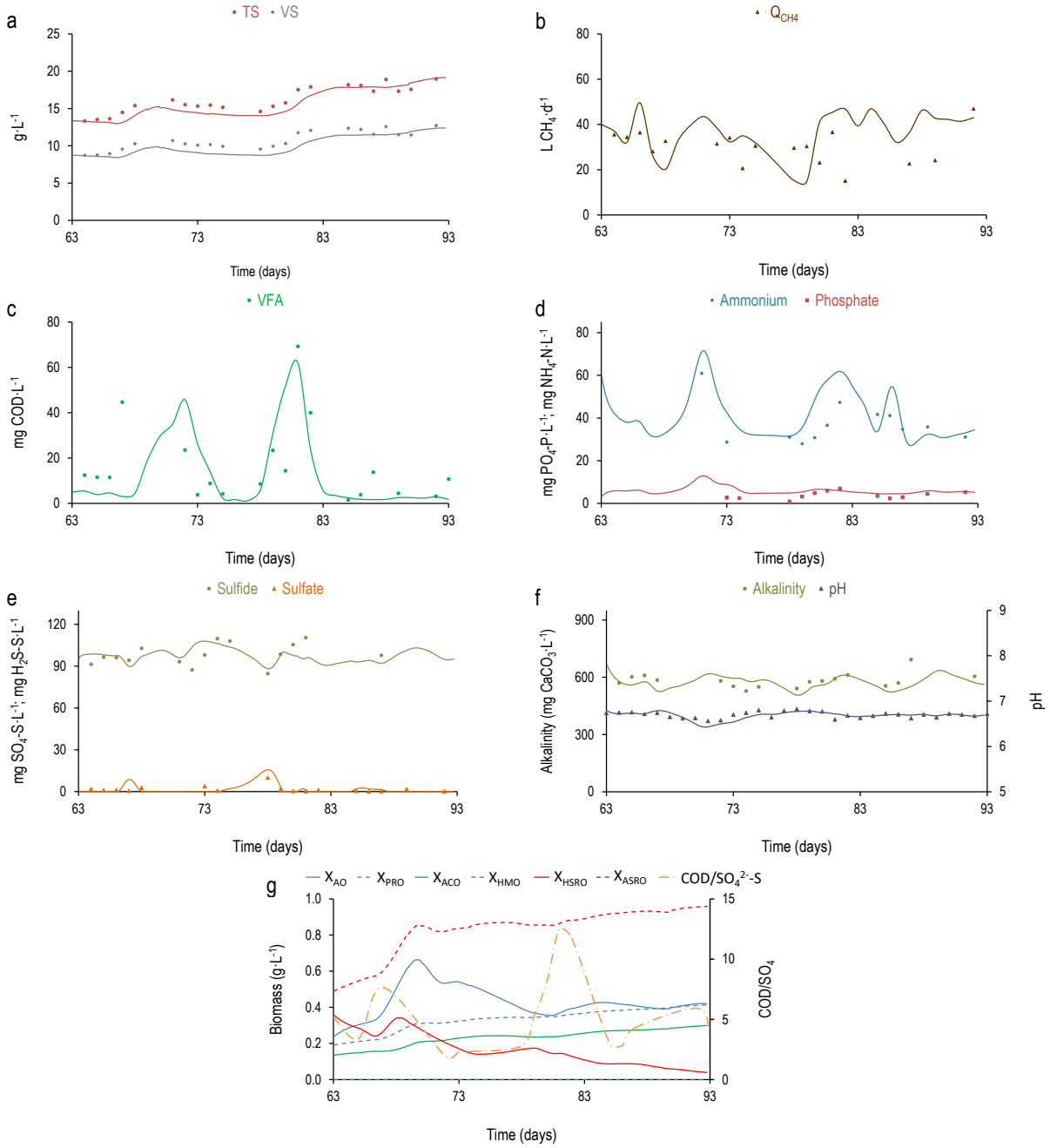

Figure 3. Dynamic simulation of period II (SRT of 70 days, temperature of 33 ºC and HRT of 17 to 11 hours). Evolution of: (a) VS, and TS in the mixed liquor; (b) methane production; (c) VFA concentration in the mixed liquor; (d) ammonium and phosphate in the mixed liquor; (e) sulfide and sulfate in the effluent; (f) alkalinity and pH in the mixed liquor; and (g) COD/SO_4^{-2}-S ratio and microbial populations (X_{AO}: acidogens; X_{PRO}: acetogens; X_{ACO}: acetoclastic methanogens; X_{HMO}: Hydrogenotrophic methanogens; X_{HSRO}: heterotrophic sulfate reducers; X_{ASRO}: autotrophic sulfate reducers). (Experimental results are represented by points and model predictions are represented by continuous lines).

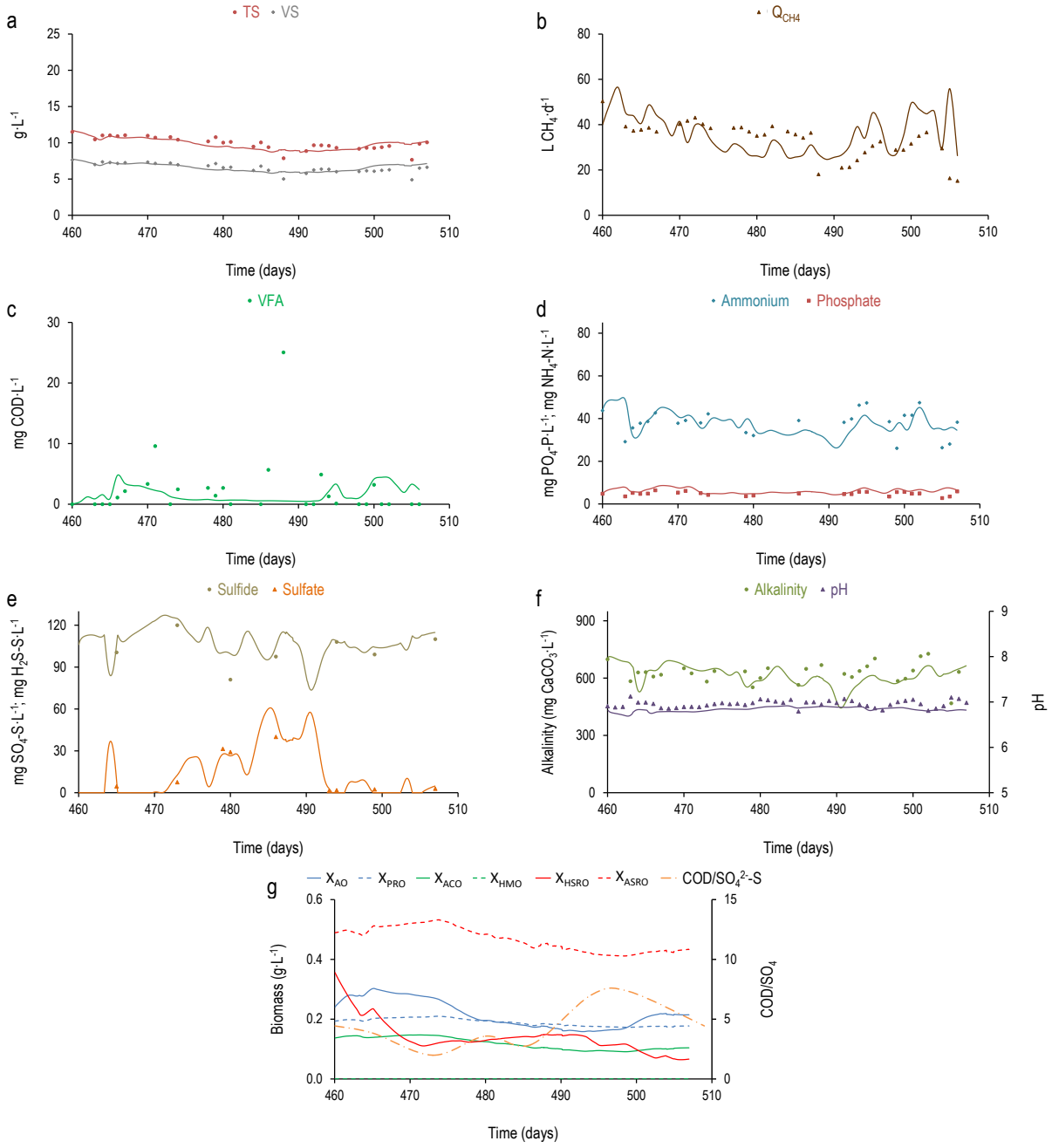

Figure 4. Dynamic simulation of period VI (SRT of 70 to 40 days, temperature of 29 ºC and HRT of 34 hours). Evolution of: (a) VS, and TS in the mixed liquor; (b) methane production; (c) VFA concentration in the mixed liquor; (d) ammonium and phosphate in the mixed liquor; (e) sulfide and sulfate in the effluent; (f) alkalinity and pH in the mixed liquor; and (g) COD/SO_4^{-2}-S ratio and microbial populations (X_{AO}: acidogens; X_{PRO}: acetogens; X_{ACO}: acetoclastic methanogens; X_{HMO}: Hydrogenotrophic methanogens; X_{HSRO}: heterotrophic sulfate reducers; X_{ASRO}: autotrophic sulfate reducers). (Experimental results are represented by points and model predictions are represented by continuous lines).

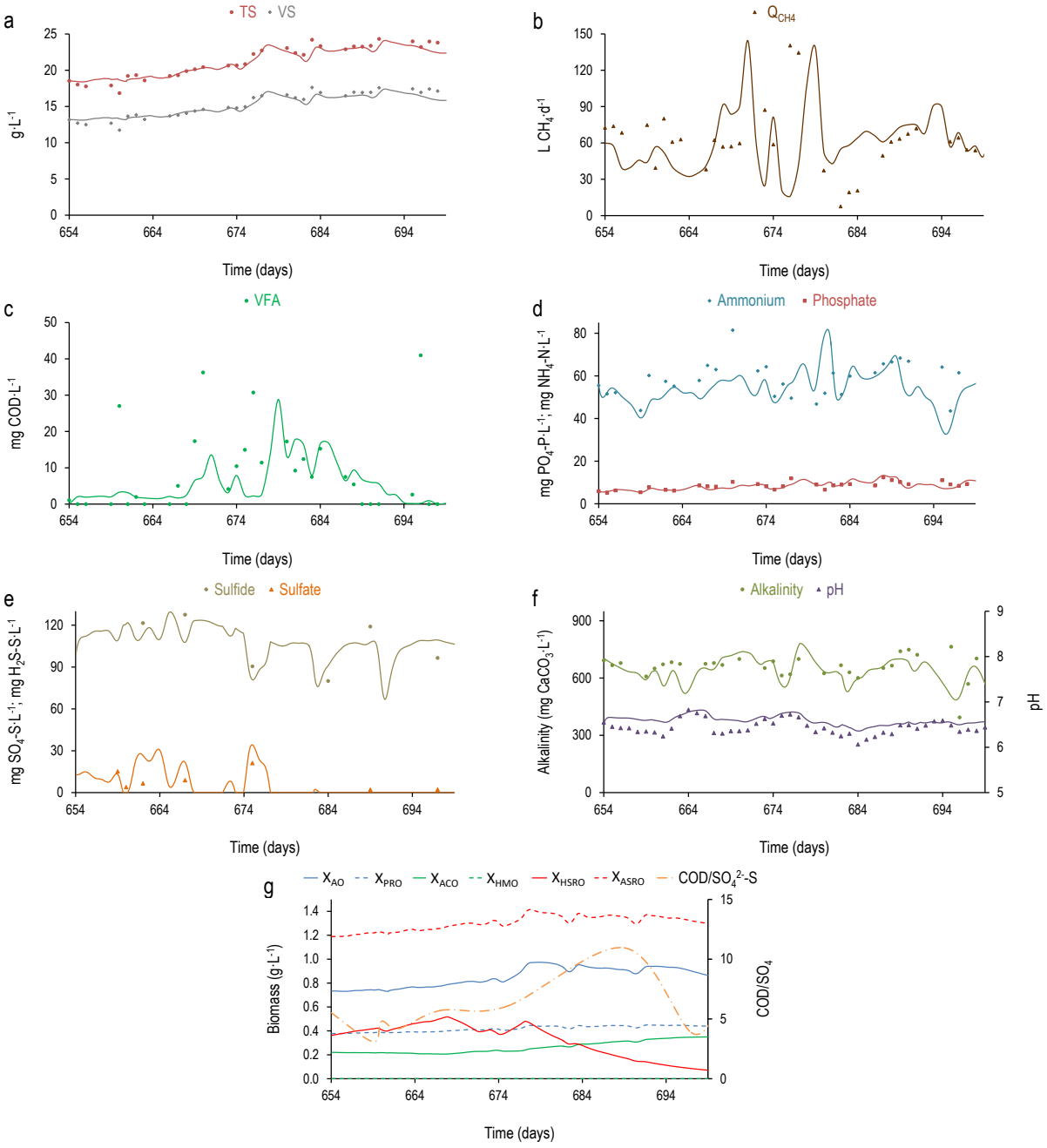

Figure 5. Dynamic simulation of period X (SRT of 30 to 40 days, temperature of 20.5 ºC and HRT of 15 hours). Evolution of: (a) VS, and TS in the mixed liquor; (b) methane production; (c) VFA concentration in the mixed liquor; (d) ammonium and phosphate in the mixed liquor; (e) sulfide and sulfate in the effluent; (f) alkalinity and pH in the mixed liquor; and (g) COD/SO_4^{-2}-S ratio and microbial populations (X_{AO}: acidogens; X_{PRO}: acetogens; X_{ACO}: acetoclastic methanogens; X_{HMO}: Hydrogenotrophic methanogens; X_{HSRO}: heterotrophic sulfate reducers; X_{ASRO}: autotrophic sulfate reducers). (Experimental results are represented by points and model predictions are represented by continuous lines).

Table 1. Average influent characterization during the experimental period.

Parameter	Units	Mean	SD*
COD_T	$mg \cdot L^{-1}$	597.9	266.2
COD_S	$mg \cdot L^{-1}$	83.3	22.0
BOD_T	$mg \cdot L^{-1}$	391.4	140.8
BOD_S	$mg \cdot L^{-1}$	64.3	19.7
VFA	$mg\ COD \cdot L^{-1}$	8.1	7.9
Ammonium	$mg\ NH_4^+\text{-}N \cdot L^{-1}$	32.8	9.0
Phosphate	$mg\ PO_4^{3-}\text{-}P \cdot L^{-1}$	4.1	1.7
Sulfate	$mg\ SO_4^{2-}\text{-}S \cdot L^{-1}$	108.3	20.0
TSS	$mg \cdot L^{-1}$	312.4	181.6
VSS	$mg \cdot L^{-1}$	250.9	146.9
Alkalinity	$mg\ CaCO_3 \cdot L^{-1}$	337.7	64.5

*Standard deviation

Table 2. Stoichiometric and kinetic parameters (20°C).

Symbol	Parameter	Default value	Units	Source
Anaerobic hydrolysis by X_{AO}				
$q_{AO,XCB\_SF,hyd}$	Maximum hydrolysis rate	28.58	d^{-1}	Calibrated
$\theta_{hyd,AO}$	Arrhenius equation coefficient for $q_{AO,XCB\_SF,hyd}$	1.066	Dimensionless	Calibrated
$K_{XCB,AO}$	Half saturation value for XC_B	194.5	mg COD·L^{-1}	Calibrated
$f_{SU\_XCB,hyd}$	Yield of S_U generated	0.003	Dimensionless	Calibrated
Acidogenic bacteria (X_{AO})				
$\mu_{AO,Max}$	Monod maximum specific growth rate	1.56	d^{-1}	Calibrated
$\theta_{\mu,AO}$	Arrhenius equation coefficient for $\mu_{AO,Max}$	1.033	Dimensionless	Calibrated
b_{AO}	First order decay rate	0.122	d^{-1}	Calibrated
$\theta_{b,AO}$	Arrhenius equation coefficient for b_{AO}	1.066	Dimensionless	Calibrated
$K_{SF,AO}$	Half saturation value for S_F	5.4	mg COD·L^{-1}	Calibrated
$K_{I,Ac,AO}$	50% inhibitory value for S_{Ac}	6500	mg COD·L^{-1}	Serralta, 2004
$K_{I,H2,AO}$	50% inhibitory value for H_2	4.26272	mg COD·L^{-1}	Siegrist *et al.*, 1993
$K_{I,[H2S],AO}$	50% inhibitory value for H_2S	257	mg H_2S-S·L^{-1}	Fedorovich *et al.*, 2003
$K_{S,H,AO}$	Half saturation value for pH	0.0000002	mol H^+·L^{-1}	Serralta, 2004
$K_{I,H,AO}$	50% inhibitory value for pH	0.00435	mol H^+·L^{-1}	Serralta, 2004
Y_{AO}	Yield of biomass on substrate X_{AO}	0.142	mg COD·mg^{-1} COD	Calibrated
$f_{XU\_AO,lys}$	Yield of X_U generated during decay	0.2	Dimensionless	Siegrist et al., 2002
$f_{SF\_Ac,AO}$	Yield of S_F transformed in S_{Ac}	0.274	Dimensionless	Calibrated
$f_{SF\_VFA,AO}$	Yield of S_F transformed in S_{VFA}	0.401	Dimensionless	Calibrated
Acetogenic bacteria (X_{PRO})				
$\mu_{PRO,Max}$	Monod maximum specific growth rate	1.59	d^{-1}	Calibrated
$\theta_{\mu,PRO}$	Arrhenius equation coefficient for $\mu_{PRO,Max}$	1.043	Dimensionless	Calibrated
b_{PRO}	First order decay rate	0.015	d^{-1}	Calibrated
$\theta_{b,PRO}$	Arrhenius equation coefficient for b_{PRO}	1.032	Dimensionless	Calibrated
$K_{VFA,PRO}$	Half saturation value for S_{VFA}	2.2	mg COD·L^{-1}	Calibrated
$K_{I,Ac,PRO}$	50% inhibitory value for S_{Ac}	1500	mg COD·L^{-1}	Siegrist et al., 1993
$K_{I,H2,PRO}$	50% inhibitory value for H_2	0.66939	mg COD·L^{-1}	Siegrist et al., 1993
$K_{I,[H2S],PRO}$	50% inhibitory value for H_2S	257	mg H_2S-S·L^{-1}	Fedorovich et al., 2003
$K_{S,H,PRO}$	Half saturation value for pH	0.00001	mol H^+·L^{-1}	Siegrist et al., 1993
$K_{I,H,PRO}$	50% inhibitory value for pH	0.00063	mol H^+·L^{-1}	Siegrist et al., 1993
Y_{PRO}	Yield of biomass on substrate	0.061	mg COD·mg^{-1} COD	Calibrated
$f_{XU\_PRO,lys}$	Yield of X_U generated during decay	0.2	Dimensionless	Siegrist et al., 2002
$f_{VFA\_Ac,PRO}$	Yield of S_{VFA} transformed in S_{Ac}	0.258	Dimensionless	Calibrated
Methanogenic acetoclastic organisms (X_{ACO})				
$\mu_{ACO,Max}$	Monod maximum specific growth rate	0.20	d^{-1}	Calibrated
$\theta_{\mu,ACO}$	Arrhenius equation coefficient for $\mu_{ACO,Max}$	1.031	Dimensionless	Calibrated
b_{ACO}	First order decay rate	0.010	d^{-1}	Calibrated
$\theta_{b,ACO}$	Arrhenius equation coefficient for b_{ACO}	1.076	Dimensionless	Calibrated
$K_{Ac,ACO}$	Half saturation value for S_{Ac}	7.2	mg COD·L^{-1}	Calibrated
$K_{I,[H2S],ACO}$	50% inhibitory value for H_2S	245	mg H_2S-S·L^{-1}	Fedorovich et al., 2003
$K_{S,H,ACO}$	Half saturation value for pH	0.00001	mol H^+·L^{-1}	Siegrist et al., 1993
$K_{I,H,ACO}$	50% inhibitory value for pH	0.00063	mol H^+·L^{-1}	Siegrist et al., 1993
Y_{ACO}	Yield of biomass on substrate	0.054	mg COD·mg^{-1} COD	Calibrated
$f_{XU\_ACO,lys}$	Yield of X_U generated during decay	0.20	Dimensionless	Siegrist et al., 2002
Methanogenic hydrogenotrophic organisms (X_{HMO})				

Symbol	Parameter	Default value	Units	Source
$\mu_{HMO,Max}$	Monod maximum specific growth rate	0.81	d^{-1}	Calibrated
$\theta_{\mu,HMO}$	Arrhenius equation coefficient for $\mu_{HMO,Max}$	1.030	Dimensionless	Calibrated
b_{HMO}	First order decay rate	0.152	d^{-1}	Calibrated
$\theta_{b,HMO}$	Arrhenius equation coefficient for b_{HMO}	1.064	Dimensionless	Calibrated
$K_{H2,HMO}$	Half saturation value for H_2	0.889	mg COD·L^{-1}	Calibrated
$K_{Ig,C,HMO}$	Half saturation value for $S_{Ig,C}$	0.000005	mol C·L^{-1}	Henze et al., 1999 *
$K_{I,[H2S],HMO}$	50% inhibitory value for H_2S	213	mg H_2S-S·L^{-1}	Fedorovich et al., 2003
$K_{S,H,HMO}$	Half saturation value for pH	0.00001	mol H^+·L^{-1}	Siegrist et al., 1993
$K_{I,H,HMO}$	50% inhibitory value for pH	0.00063	mol H^+·L^{-1}	Siegrist et al., 1993
Y_{HMO}	Yield of biomass on substrate	0.021	mg COD·mg^{-1} COD	Calibrated
$f_{XU\_HMO,lys}$	Yield of X_U generated during decay	0.2	Dimensionless	Siegrist et al., 2002
Autotrophic sulfate-reducing organisms (X_{ASRO})				
$\mu_{ASRO,Max}$	Monod maximum specific growth rate	1.43	d^{-1}	Calibrated
$\theta_{\mu,ASRO}$	Arrhenius equation coefficient for $\mu_{ASRO,Max}$	1.100	Dimensionless	Calibrated
b_{ASRO}	First order decay rate X_{ASRO}	0.021	d^{-1}	Calibrated
$\theta_{b,ASRO}$	Arrhenius equation coefficient for b_{ASRO}	1.066	Dimensionless	Calibrated
$K_{SO4,ASRO}$	Half saturation value for SO_4^{2-}	0.25	mg SO_4-S·L^{-1}	Calibrated
$K_{H2,ASRO}$	Half saturation value for H_2	0.100	mg COD·L^{-1}	Calibrated
$K_{Ig,C,ASRO}$	Half saturation value for $S_{Ig,C}$	0.000005	mol C·L^{-1}	Henze et al., 1999 *
$K_{I,[H2S],ASRO}$	50% inhibitory value for H_2S	265	mg H_2S-S·L^{-1}	Fedorovich et al., 2003
$K_{S,H,ASRO}$	Half saturation value for pH	0.00001	mol H^+·L^{-1}	Siegrist et al., 1993
$K_{I,H,ASRO}$	50% inhibitory value for pH	0.00063	mol H^+·L^{-1}	Siegrist et al., 1993
Y_{ASRO}	Yield of biomass on substrate	0.147	mg COD·mg^{-1} COD	Calibrated
$f_{XU\_ASRO,lys}$	Yield of X_U generated during decay	0.2	Dimensionless	Siegrist et al., 2002
Heterotrophic sulfate-reducing organisms (X_{HSRO})				
$\mu_{HSRO,Max}$	Monod maximum specific growth rate	0.62	d^{-1}	Calibrated***
$\theta_{\mu,HSRO}$	Arrhenius equation coefficient for $\mu_{HSRO,Max}$	1.077	Dimensionless	Calibrated***
b_{HSRO}	First order decay rate X_{HSRO}	0.068	d^{-1}	Calibrated***
$\theta_{b,HSRO}$	Arrhenius equation coefficient for b_{HSRO}	1.067	Dimensionless	Calibrated***
$K_{SO4,HSRO}$	Half saturation value for SO_4^{2-}	9.3	mg SO_4-S·L^{-1}	Calibrated***
$K_{VFA,HSRO}$	Half saturation value for S_{VFA}	29.4	mg COD·L^{-1}	Calibrated***
$K_{Ac,HSRO}$	Half saturation value for S_{Ac}	5.12	mg COD·L^{-1}	Calibrated***
$K_{I,[H2S],HSRO}$	50% inhibitory value for H_2S	265	mg H_2S-S·L^{-1}	Fedorovich et al., 2003
$K_{S,H,HSRO}$	Half saturation value for pH	0.00001	mol H^+·L^{-1}	Siegrist et al., 1993
$K_{I,H,HSRO}$	50% inhibitory value for pH	0.00063	mol H^+·L^{-1}	Siegrist et al., 1993
Y_{HSRO}	Yield of biomass on substrate	0.362	mg COD·mg^{-1} COD	Calibrated***
$f_{XU\_HSRO,lys}$	Yield of X_U generated during decay	0.2	Dimensionless	Siegrist et al., 2002
General parameters				
K_{NHx}	Half saturation value (catabolism only) for NH_4^+	0.05	mg NH_4-N·L^{-1}	Henze et al., 1999 **
K_{PO4}	Half saturation value (catabolism only) for PO_4^{3-}	0.01	mg PO_4-P·L^{-1}	Henze et al., 1999 **

*Autotrophs. ** Heterotrophs. *** Off line experiments

Table 3. Simulation results for the pseudo-steady state reached at the end of period VI (SRT of 40 days, temperature of 29 ºC and HRT of 34 hours), period IX (SRT of 30 days, temperature of 20 ºC and HRT of 17.5 hours), period X (SRT of 40 days, temperature of 20.5 ºC and HRT of 15 hours) and period XII (SRT of 20 days, temperature of 27.3 ºC and HRT of 14 hours).

Stream	Parameter	*PERIOD VI*			*PERIOD IX*			*PERIOD X*			*PERIOD XII*		
		Experimental		Modelled	Experimental		Modelled	Experimental		Modelled	Experimental		Modelled
		Mean	SD*	Mean	Mean	SD*	Mean	Mean	SD*	Mean	Mean	SD*	Mean
Effluent	COD_S ($mg \cdot L^{-1}$)	76.8	40.1	76.8	73.1	4.5	75.3	102.6	14.3	102.9	82.2	29.2	78.8
	VFA ($mg\ COD \cdot L^{-1}$)	<LQ		<LQ	<LQ		2.4	<LQ		2.0	<LQ		3.0
	Ammonium ($mg\ NH_4^+\text{-}N \cdot L^{-1}$)	38.3	7.1	38.3	55.0	9.4	52.8	62.3	8.0	55.4	42.6	10.1	47.3
	Phosphate ($mg\ PO_4^{3-}\text{-}P \cdot L^{-1}$)	4.91	1.02	4.91	6.95	1.55	6.90	9.94	1.36	8.7	6.87	1.45	8.70
	Sulfate ($mg\ SO_4^{2-}\text{-}S \cdot L^{-1}$)	< LQ		< LQ	4.6	2.3	3.5	<LQ		2.1	10.7	10.4	2.1
	Sulfide ($mg\ H_2S\text{-}S \cdot L^{-1}$)	102.7	4.7	102.7	111.4	21.8	114.6	107.8	15.9	107.8	101.7	14.7	112.3
Sludge	COD_T ($mg \cdot L^{-1}$)	10547	694	10547	22117	512	22383	28763	566	28789.6	14503	639	14319
	TSS ($mg \cdot L^{-1}$)	9424	572	9424	18347	402	18367	23563	469	23543.9	12346	512	12337
	VSS ($mg \cdot L^{-1}$)	6182	415	6182	13123	307	13047	17091	339	17091.8	8551	382	8553
	Alkalinity ($mg\ CaCO_3 \cdot L^{-1}$)	648	75	648	669	50	653	662	117	599.6	635	94	638
Biogas	CH_4 production ($L \cdot d^{-1}$)	36.1	28.7	36.1	22.6	22.6	41.4	115.6	38.0	120.6	13.5	13.5	14.0

* Standard Deviation